

Impact of DC Voltage Droop Control Structures on DC Oscillations in a MTDC

F. Thams

Technical University of Denmark (DTU)
Center for Electric Power and Energy
Email: fltha@elektro.dtu.dk

S. Chatzivasileiadis

Technical University of Denmark (DTU)
Center for Electric Power and Energy
Email: spchatz@elektro.dtu.dk

E. Prieto-Araujo

Technical University of Catalonia
CITCEA, Barcelona, Spain
Email: eduardo.prieto-araujo@citcea.upc.edu

R. Eriksson

Swedish National Grid
Markets and System Development
Email: errobban@gmail.com

Introduction: Offshore wind farms raised the interest in HVDC transmission based on voltage source converter (VSC-HVDC). It is the most appropriate technology for a multi-terminal HVDC (MTDC) grid facilitating the change of power direction and enabling parallel connections. The control of a MTDC grid is still an open research topic.

1. Control of MTDC grid:

- Preferable to have a decentralized control structure with multiple units actively participate in the dc voltage control
- One of the preferred control structures (CSs) is dc voltage droop control.
- However, in technical literature several alternative droop control schemes have been discussed.
- They can be categorized by eight different types of structures
- Comparable tuning for all control structures with a settling time of 100ms achieved by using robust control techniques
- Comparable power / current based droop gains [1]: $k_{droop,i} = \frac{V_{dc}^*}{\frac{1}{k_{droop,p}} - I_{dc}^*/q}$

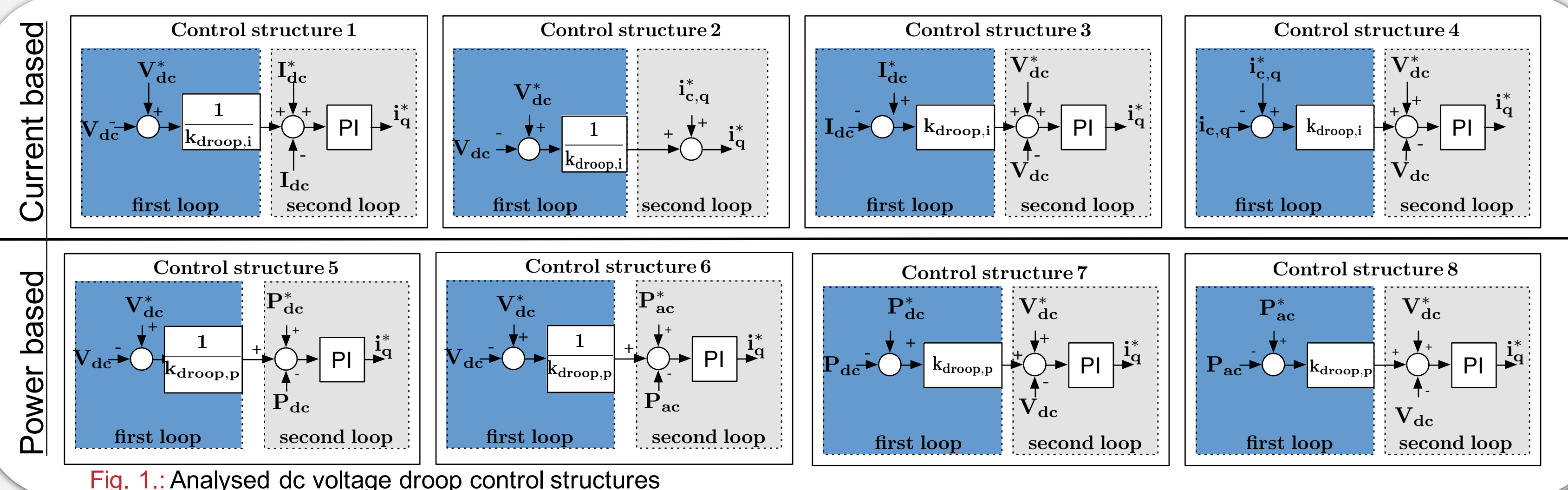


Fig. 1.: Analysed dc voltage droop control structures

2. Model:

- 3 terminal grid with two grid side converters (GSCs)
- GSCs connected by LC filters to two different equivalent ac grids modeled as Thévenin equivalent.

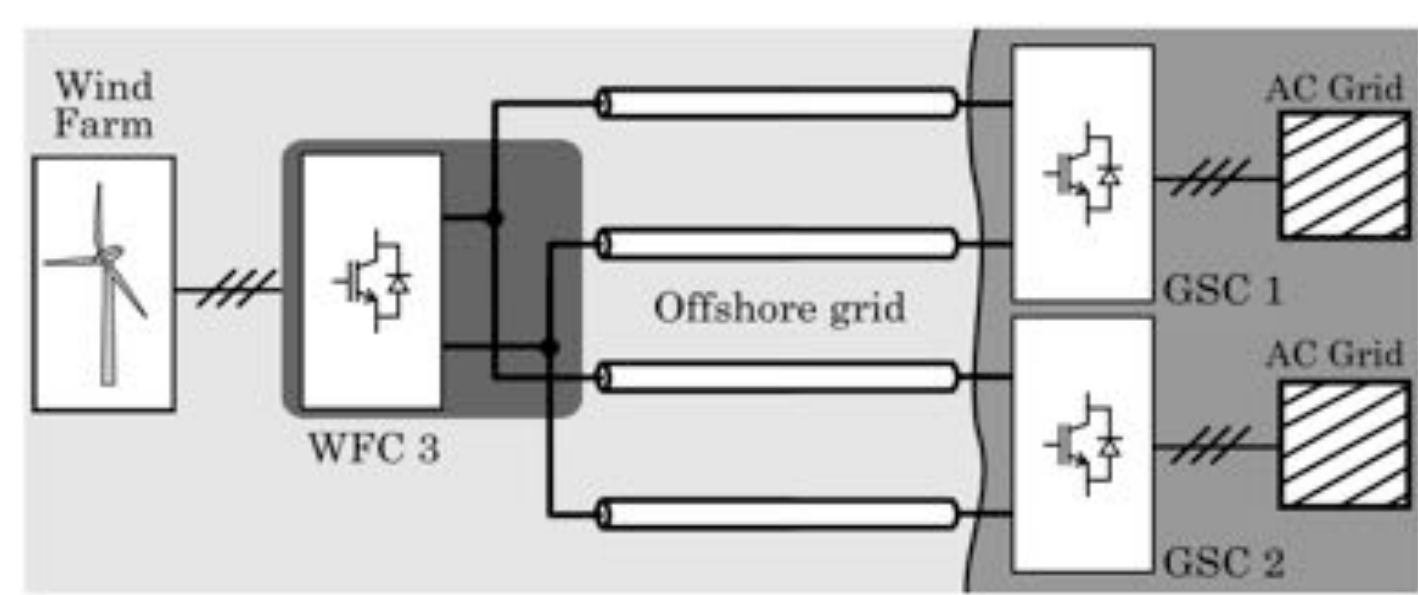


Fig. 2.: MTDC grid

- Conventional current controller in SRF tuned by Internal Model Control (IMC) technique with a settling time of 10ms
- Saturation limits included
- DC lines are modeled using a single π -equivalent model
- Closed loop transfer function matrices considering ac and dc dynamics: $\Delta e(s) = \Delta y(s) - \Delta r(s)$

$$\Delta u_{iq} = (U_w^{uiq}(s) U_r^{uiq}(s)) (\Delta w(s) \Delta r(s))^T$$

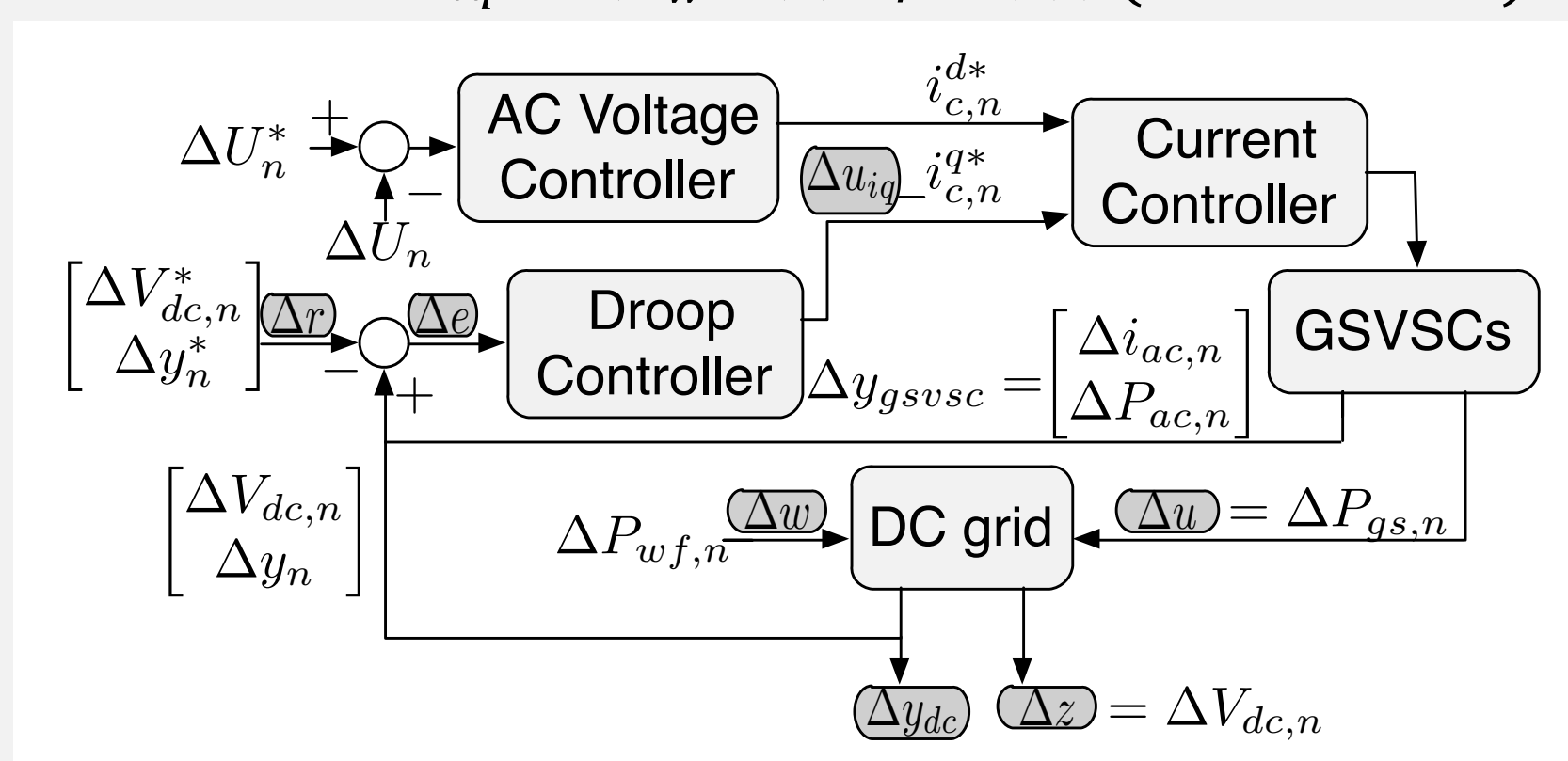


Fig. 3.: Control structure of multi-terminal HVDC grid

3. Methodology:

- Performance of the CSs is analyzed by the singular value representation (SV) of the system transfer function matrix $\sigma_i(E_w(j\omega)) = \sqrt{\lambda_i(E_w^T(j\omega)E_w(j\omega))}$
- The maximum SV indicates the maximum amplification of the corresponding inputs (P_{wf}) by the system seen from a specific output (ΔV_{dc}).
- The max. gain of SV for max. voltage error of 10% of the nominal value at each terminal is calculated as [2]: $\bar{\sigma}(E_w(0)) \leq \frac{\|e(0)\|_2}{\|w(0)\|_2} = 20 \log_{10} \left(\frac{\sqrt{e_{mx1} + e_{mx2}}}{P_3} \right) = -81.85 \text{ dB}$
- Max. allowed current flowing through the converter = 110% of the nominal current value (represents the control action) [2]: $\sigma(U_w^{uiq}(0)) \leq -109.74 \text{ dB}$

4. Results: Both GSCs use same CS

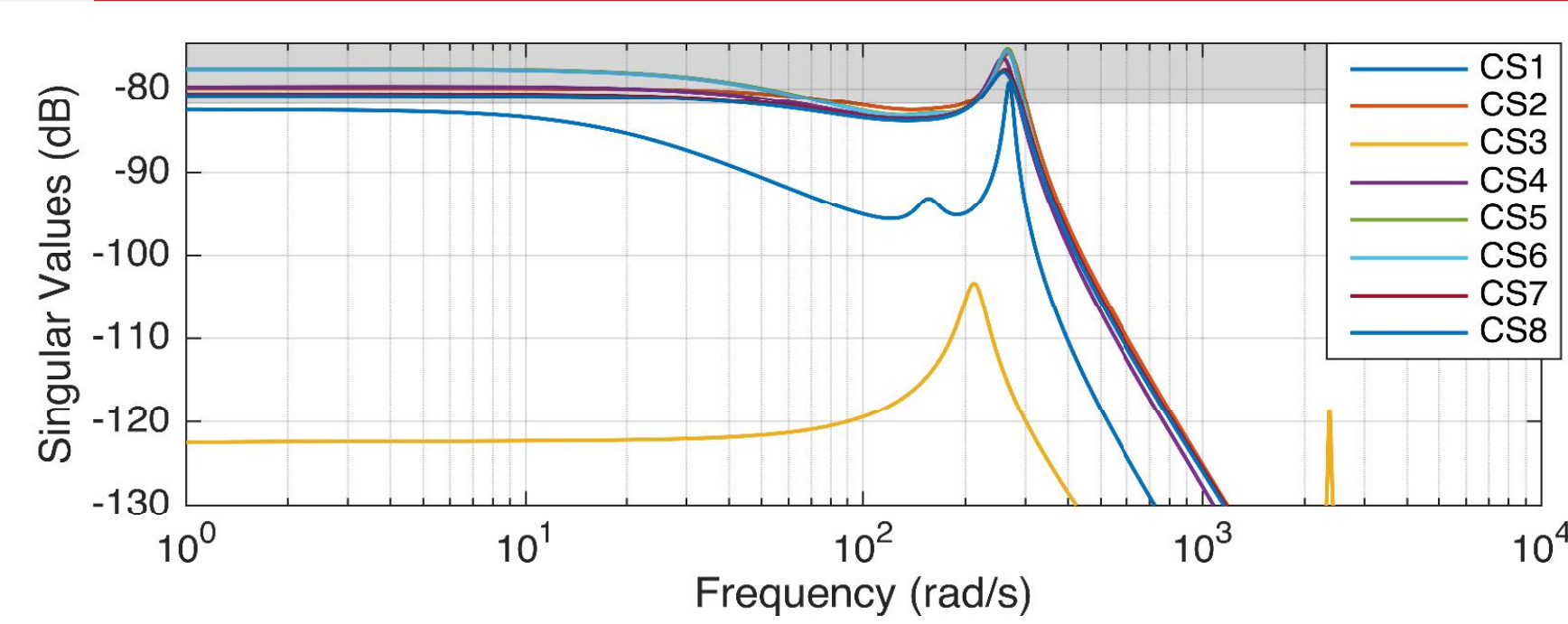


Fig. 4.: Singular value representation of $E_w(j\omega)$ (dc voltage error - wind power input) for the case where both GSCs use the same CS

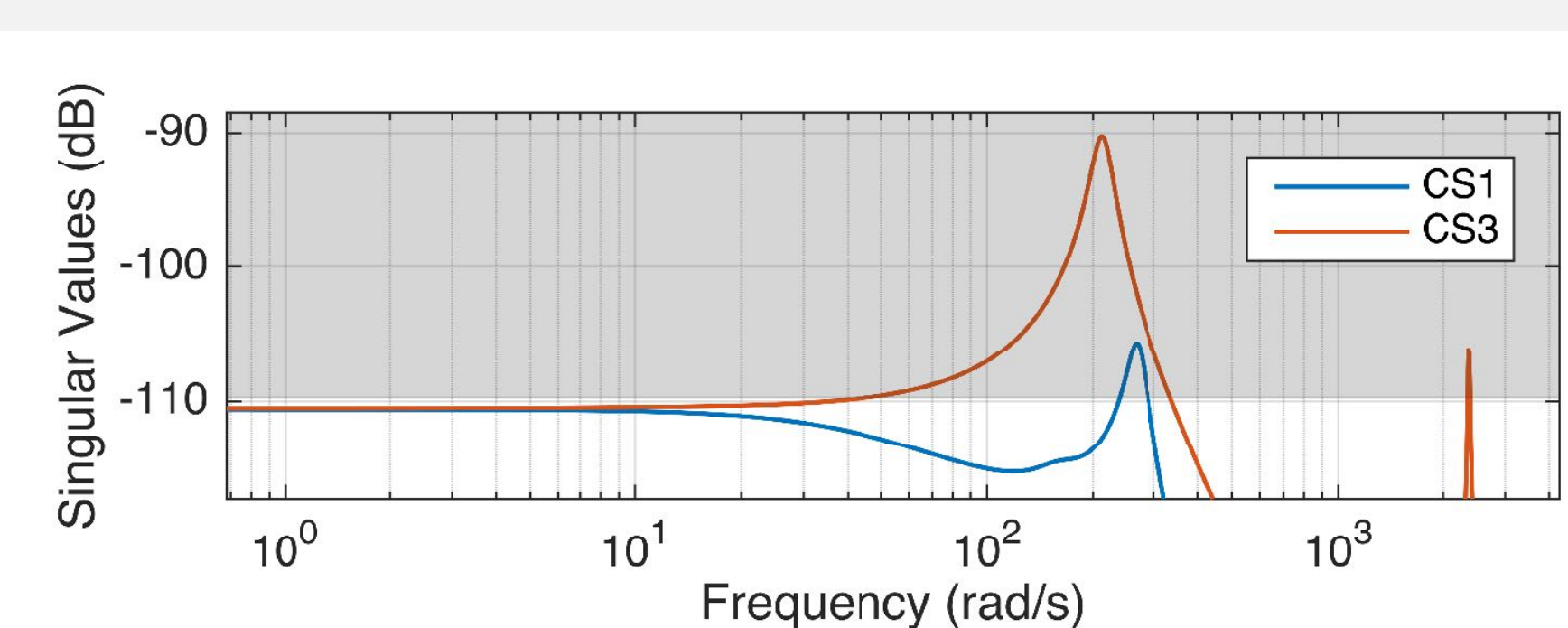


Fig. 5.: Singular value representation of $U_w^{uiq}(j\omega)$ (current controller references - wind power input) for the case where both GSCs use the same CS - results of CS1 comparable to CS2,4-8

- CS3 ($I_{dc} - V_{dc}$) achieves significantly lower singular values at costs of higher control action for $\omega > 10 \frac{rad}{s}$
- CS1 ($V_{dc} - I_{dc}$) fulfils the maximum gain requirement in steady state, but not for the whole frequency range - but same control action as remaining CSs
- CS2,4-8 do not even fulfil maximum gain requirement
- If power spectrum of wind farm includes frequency of resonance peaks: $\Delta V_{dc} > 10\% V_{dc,n}$ or $I_{conv} > 110\% I_N$

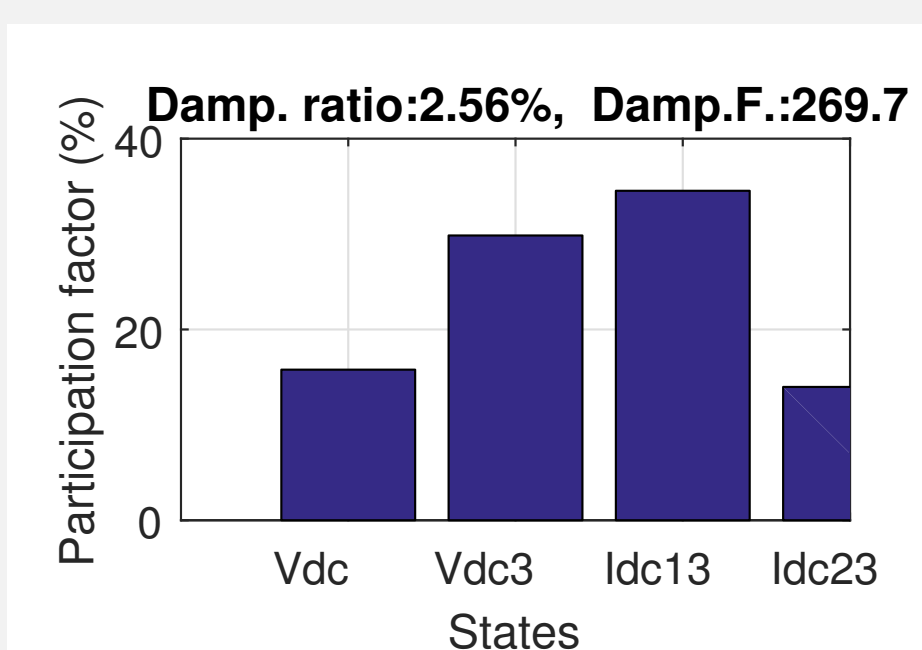
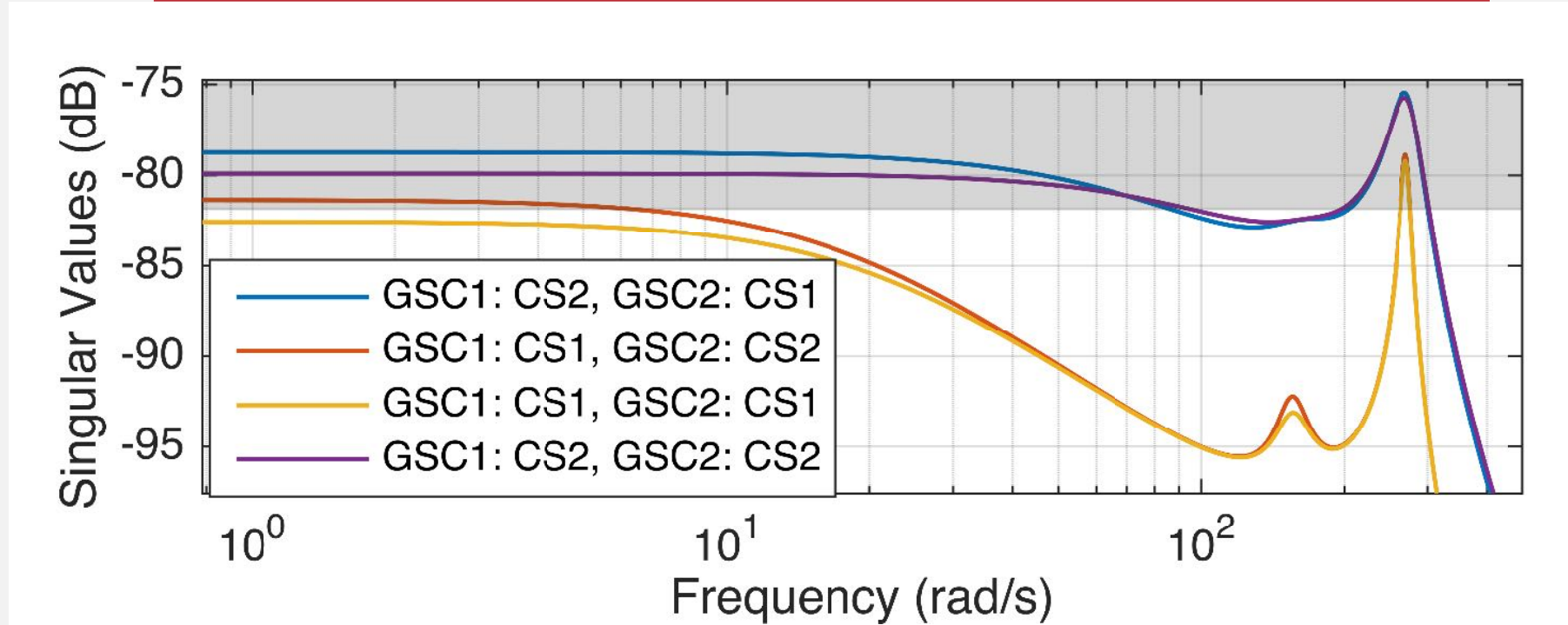


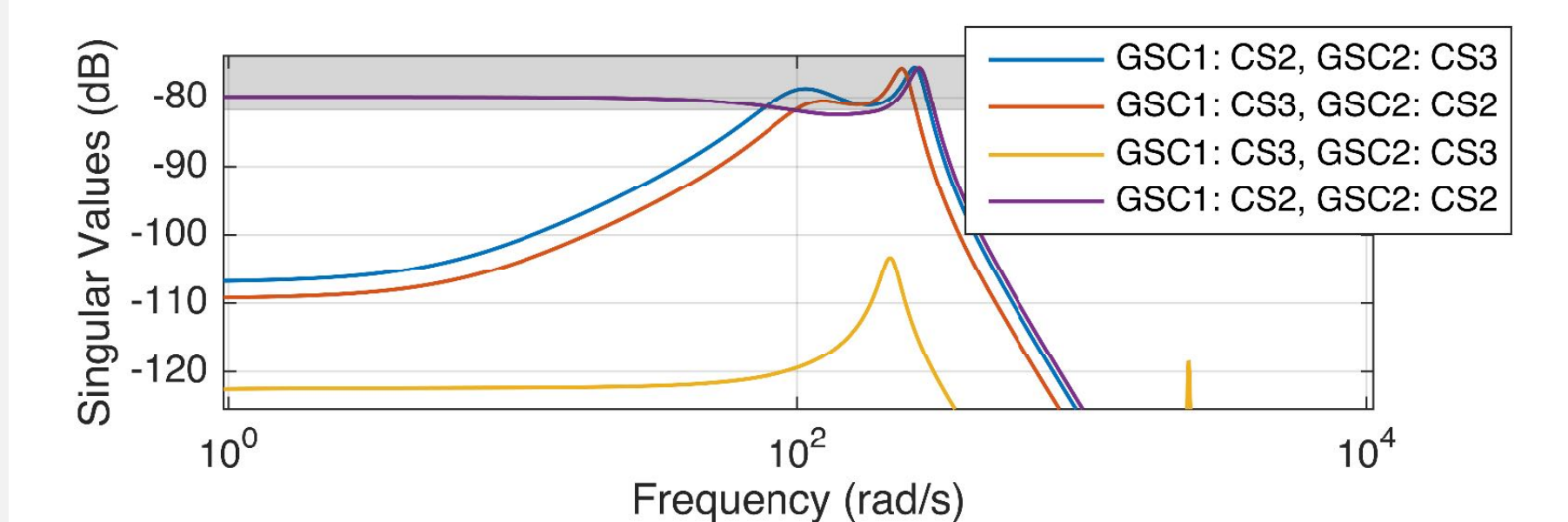
Fig. 6.: Participation factor analysis of the eigenvalues of $E_w(j\omega)$ with damping frequency corresponding to the resonance peak for the case where both GSCs use CS1 ($V_{dc} - I_{dc}$)

- Origin of resonance peaks determined by participation factor analysis: related to dc values (voltage / current) at the wind farm

5. Results: GSCs use different CS



a) Control structure 1 ($V_{dc} - I_{dc}$) and control structure 2 ($V_{dc} - I_{dc}$)



b) Control structure 3 ($V_{dc} - I_{dc}$) and control structure 2 ($V_{dc} - I_{dc}$)

Fig. 7.: Singular value representation of $E_w(j\omega)$ (dc voltage error - wind power input) for the case where both GSCs use different CS

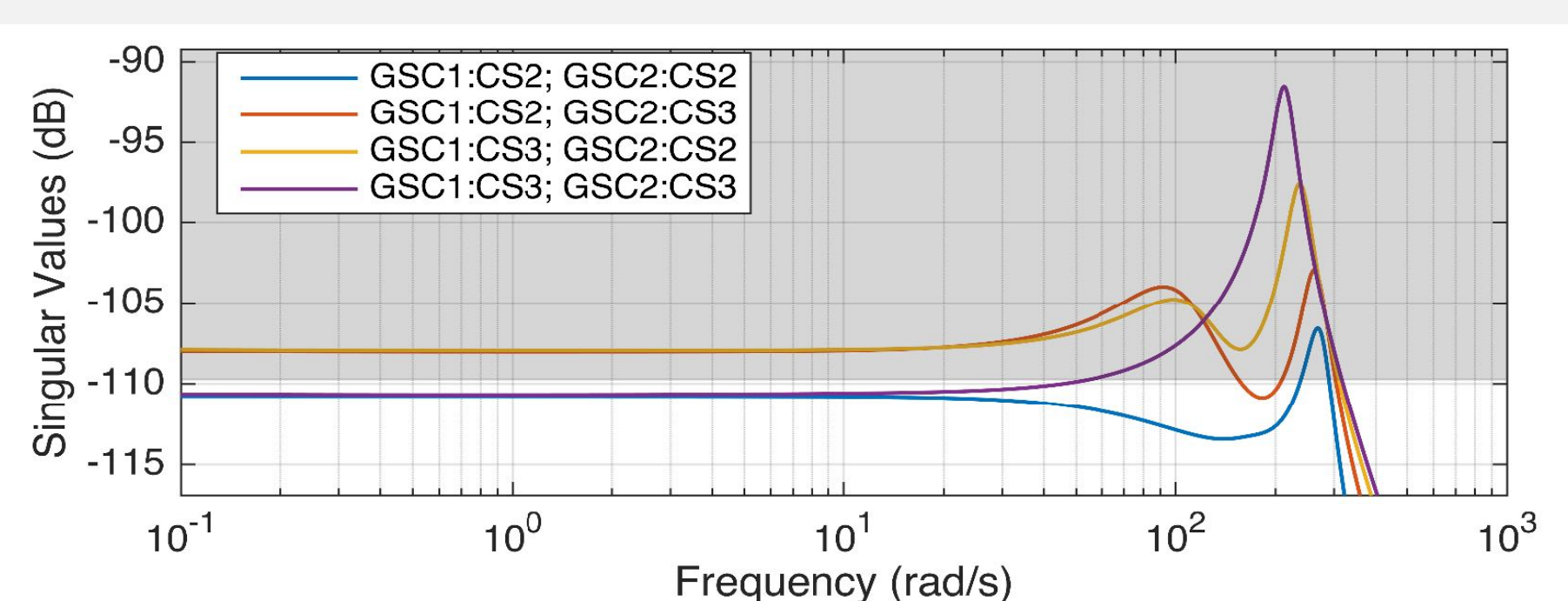


Fig. 8.: Singular value representation of $U_w^{uiq}(s)$ (current loop references - wind power input) for a combination of CS2 and CS3

- For all CSs except CS3 ($I_{dc} - V_{dc}$): CS at GSC closer to WFC dominates SV representation (Fig. 7a)
- CS3 ($I_{dc} - V_{dc}$) leads to significant lower SV in steady state, but does not improve damping of resonance peaks (Fig. 7b)
- Better damping of CS3 ($I_{dc} - V_{dc}$) comes at the cost of increased control action (Fig. 8)
- Combination of any CS with CS3 increases control action already in steady state

5. Conclusion

- All CSs need damping of dc oscillations / control actions in order to comply with boundaries over whole frequency range
- Closeness of GSCs to uncontrolled node (wind farm) needs to be considered in design of MTDC
- Current damping solutions focus on damping at GSC
- In this work, we show the need for development of appropriate damping of dc oscillations at wind farm converter